RESEARCH ARTICLE

Functional classification of gill ionocytes and spatiotemporal changes in their distribution after transfer from seawater to freshwater in Japanese seabass

Mayu Inokuchi[1,*], Masahiro Nakamura[2], Hiroshi Miyanishi[3], Junya Hiroi[4] and Toyoji Kaneko[5]

ABSTRACT

Spatiotemporal changes in branchial ionocyte distribution were investigated following transfer from seawater (SW) to freshwater (FW) in Japanese seabass. The mRNA expression levels of cystic fibrosis transmembrane conductance regulator (CFTR) and $Na^+/K^+/2Cl^-$ cotransporter 1a (NKCC1a) in the gills rapidly decreased after transfer to FW, whereas Na^+/H^+ exchanger 3 (NHE3) and Na^+/Cl^- cotransporter 2 (NCC2) expression were upregulated following the transfer. Using quadruple-color whole-mount immunofluorescence staining with anti-Na^+/K^+-ATPase, anti-NHE3, anti-CFTR and T4 (anti-NKCC1a/NCC2) antibodies, we classified ionocytes into one SW type and two FW types: NHE3 cell and NCC2 cell. Time course observation after transfer revealed an intermediate type between SW-type and FW-type NHE3 ionocytes, suggesting functional plasticity of ionocytes. Finally, on the basis of the ionocyte classification of Japanese seabass, we observed the location of ionocyte subtypes on frozen sections of the gill filaments stained by triple-color immunofluorescence staining. Our observation indicated that SW-type ionocytes transformed into FW-type NHE3 ionocytes and at the same time shifted their distribution from filaments to lamellae. However, FW-specific NCC2 ionocytes appeared mainly in the filaments. Taken together, these findings indicate that ionocytes originated from undifferentiated cells in the filaments and expanded their distribution to the lamellae during FW acclimation.

KEY WORDS: Ionocyte, Gill, Osmoregulation, Japanese seabass, Filament, Lamella

INTRODUCTION

Osmoregulation is essential for maintaining internal homeostasis to ensure the normal operation of cell functions and activities. In teleost fishes, as in most vertebrates, plasma osmolality is maintained within narrow physiological ranges, equivalent to about one-third of seawater (SW) osmolality. Osmoregulation in teleosts is achieved by integrated ion- and water-transporting functions of the gills, kidney and intestine (Marshall and Grosell, 2006). In particular, ionocytes (also known as chloride cells or mitochondrion-rich cells) in the gills are important osmoregulatory sites for maintaining ionic balance in fish, being responsible for ion uptake in freshwater (FW) and ion secretion in SW (Hwang and Lin, 2013).

The function of ionocytes is determined by the localization of various ion-transporting proteins in the apical and basolateral membranes. Among the ion-transporting proteins, Na^+/K^+-ATPase (NKA) is a key enzyme in ionoregulatory functions of ionocytes, creating ionic and electronic gradients across the plasma membrane, and thus providing the driving force for ion transport in both FW and SW. The currently accepted model proposes that active ion secretion from ionocytes in fish acclimated to SW is mediated by NKA and $Na^+/K^+/2Cl^-$ cotransporter 1a (NKCC1a) in the basolateral membrane, and by the Cl^- channel, cystic fibrosis transmembrane conductance regulator (CFTR), in the apical membrane (Hwang and Lin, 2013). The SW-type ionocytes frequently form multicellular complexes with accessory cells. These ionocytes are referred to as type IV ionocytes in Mozambique tilapia *Oreochromis mossambicus* (Hiroi et al., 2005, 2008). By contrast, the mechanisms for ion uptake in ionocytes of FW-acclimated teleosts vary according to species (Hwang and Lin, 2013). In euryhaline Mozambique tilapia and medaka *Oryzias latipes*, two distinct types of ionocytes have been considered to be responsible for ion uptake in FW: the first type is characterized by Na^+/Cl^- cotransporter 2 (NCC2) localized in the apical membrane, being referred to as type II cell in tilapia and NCC cell in medaka; the second type of FW ionocytes is characterized by the presence of Na^+/H^+ exchanger 3 (NHE3) instead of NCC2 in the apical membrane, which is referred to as type III in tilapia and NHE cell in medaka (Hiroi et al., 2008; Inokuchi et al., 2008; Hsu et al., 2014).

Japanese seabass *Lateolabrax japonicus* is a euryhaline marine fish inhabiting coastal areas and estuaries in Japan and Korea (Islam et al., 2011). As is the case with other marine teleosts, eggs are spawned in SW. During the early part of the juvenile period, this species migrates from open water areas into estuaries (Kinoshita et al., 1995). It has been reported that some of the early juveniles ascend the river while others reside in the lower estuary or in the littoral zone (Fuji et al., 2010). One possible reason for this migration to the river is prey abundance (Fujita et al., 1988; Fuji et al., 2010).

In SW-acclimated Japanese seabass, NKA-immunopositive ionocytes were detected only in gill filaments, whereas ionocytes emerged at the proximal part of lamellae and thereafter spread over the lamellar epithelium following FW transfer (Hirai et al., 1999). These findings suggested that Japanese seabass ionocytes emerged in the gill lamellae after FW transfer, and that those lamellar ionocytes originated from the gill filaments and migrated to the lamellae during FW acclimation (Hirai et al., 1999). A salinity-induced change in the distributional pattern of ionocytes has been

[1]Department of Life Sciences, Toyo University, Itakura, Gunma 374-0193, Japan.
[2]National Research Institute of Fisheries and Environment of Inland Sea, Fisheries Research Agency, Imabari, Ehime 794-2305, Japan. [3]Faculty of Agriculture, University of Miyazaki, Gakuen-kibanadai-nishi, Miyazaki 889-2192, Japan.
[4]Department of Anatomy, St Marianna University School of Medicine, Kawasaki, Kanagawa 216-8511, Japan. [5]Department of Aquatic Bioscience, Graduate School of Agricultural and Life Sciences, University of Tokyo, Bunkyo, Tokyo 113-8657, Japan.

*Author for correspondence (inokuchi@toyo.jp)

M.I., 0000-0001-6309-4567

reported in a variety of euryhaline teleost species (Hiroi and McCormick, 2012). However, the detailed mechanism for distributional change of gill ionocytes after salinity change remains to be elucidated.

In the present study, we aimed to clarify the spatiotemporal changes in ionocyte distribution in Japanese seabass following transfer from SW to FW. First, applying quadruple-color whole-mount immunofluorescence staining with anti-NKA, anti-NHE3, anti-CFTR and T4 (anti-NKCC1a/NCC2) antibodies, we classified ionocytes into one SW type and two FW types. Next, in order to investigate changes in the spatial distribution of different types of branchial ionocytes, we examined the time course changes in immunocytochemical localizations of NKA, NHE3, NKCC1a and NCC2 in the gills of fish transferred from SW to FW. Our findings indicated that ionocytes originated from undifferentiated cells in the filaments and expanded their distribution to the lamellae during FW adaptation.

MATERIALS AND METHODS
Fish
Japanese seabass (*Lateolabrax japonicas*, Cuvier) juveniles were caught in the Yura River estuary (10–27 ppt, Maizuru, Kyoto, Japan) with a seine net in June 2014. The fish were maintained in a stock tank supplied with recirculating filtered SW in Kyoto University Maizuru Fisheries Research Station for 3 days, and transported to University of Tokyo for the transfer experiment. Fish were fed three times a day to satiation with commercial pellets for flounders (Nippon Formula Feed Manufacturing Company Limited, Yokohama, Japan). Experiments were conducted according to the principles and procedures approved by the Institutional Animal Care and Use Committee of the University of Tokyo.

Transfer experiment
After the acclimation to SW for 2 weeks, the fish (total length, 59–98 mm) were exposed to 10% diluted SW for 24 h, and then transferred to FW (dechlorinated tap water). Fish were sampled at 0, 1, 3, 7 and 10 days after the initial transfer to 10% SW. Although 35 fish were used for this transfer experiment, 11 fish died after transfer. Similarly, a previous study reported that 77% of seabass survived at day 10 following transfer to FW (Hirai et al., 1999).

Sampling
After fish were anesthetized with 0.1% 2-phenoxyethanol, blood was collected from the caudal vessels with a heparinized syringe and needle. The blood plasma was separated by centrifugation and stored at −20°C. Later, plasma osmolality was measured with a vapor pressure osmometer (Wescor 5520, Logan, UT, USA). After blood sampling, gill filaments from the first gill arches, kidneys and intestines were removed from seabass and frozen in liquid nitrogen for total RNA extraction. For immunocytochemistry, the second gills were fixed in 4% paraformaldehyde (PFA) in 0.1 mol l^{-1} sodium phosphate buffer (PB, pH 7.4) for 24 h at 4°C, and stored in 70% ethanol.

cDNA cloning of CFTR, NKCC1a, NHE3, NCC1, NCC2 and EF1a
Total RNA was extracted from gill filaments and kidneys with Isogen (Nippon Gene, Tokyo, Japan). After digestion of genomic DNA with a TURBO DNA-free kit (Thermo Fisher Scientific, Waltham, MA, USA), first-strand cDNA was synthesized from the total RNA with a SuperScript III First-Strand Synthesis System (Thermo Fisher Scientific). Degenerate primer pairs were designed

to amplify conserved regions of CFTR, NKCC1a, NHE3, NCC1, NCC2 and EF1a (Table 1). The cDNA fragments of CFTR, NKCC1a, NHE3, NCC2 and EF1a were amplified by degenerate PCR with a cDNA template obtained from gill filaments, while the cDNA of NCC1 was amplified with cDNA template from kidneys. The PCR products were ligated into pGEM T-Easy vector (Promega, Madison, WI, USA) and sequenced using an ABI Prism 310 sequencer (Thermo Fisher Scientific).

Expression of NCC isoforms in different tissues
The expression of two isoforms of NCC (NCC1 and NCC2) was examined in osmoregulatory organs. Total RNA was extracted from the gill, kidney and intestine of Japanese seabass. Two micrograms of total RNA treated with a TURBO DNA-free kit (Thermo Fisher Scientific) was reverse-transcribed to first-strand cDNA using a High-Capacity cDNA Reverse Transcription Kit (Thermo Fisher Scientific). Samples were subjected to reverse-transcription polymerase chain reaction (RT-PCR) analysis with the primer sets shown in Table 1.

Real-time quantitative polymerase chain reaction
Expression levels of CFTR, NKCC1a, NHE3 and NCC2 were determined by qPCR with a LightCycler ST300 (Roche Diagnostic, Penzberg, Germany) and LightCycler FastStart DNA Master SYBR Green I (Roche Diagnostic). The cDNA was prepared from 2 µg total RNA extracted from the gill filaments. The concentration of the transcripts was calculated with reference to the parallel amplifications of known concentrations of the respective cloned PCR fragments, and the specificity of each PCR was confirmed by melting curve analysis. The data were normalized with the expression levels of EF1a mRNA measured in parallel. The primers used are shown in Table 1.

Antibodies
For immunocytochemical detection of NKA-immunoreactive ionocytes, we used α5 antibody [developed by Douglas Fambrough, and obtained from the Developmental Studies

Table 1. Primer sets used in the present study

Gene name		Primer sequence 5′ to 3′
Primer sets for molecular cloning and RT-PCR		
CFTR	Sense	CAYCACCTKGGCATGCA
	Antisense	GTGTCRTACCACATCTGG
NKCC1a	Sense	CACAAYAAMATCGAYGC
	Antisense	TTRGCYTCCCAYTCCAT
NHE3	Sense	TACCTSRTSGCCYTRTGGAT
	Antisense	CGCAGGCCACCGTAGCYCAT
NCC1	Sense	TGGGGDGTGATCCTGTACCT
	Antisense	AAGAAGTTGGAGATGATGGGAGC
NCC2	Sense	GCATGCTGAAYATYTGGGG
	Antisense	GAYCAGAGCRGCCCACCA
EF1a	Sense	GGGAAGGGGTCGTTCAAGTA
	Antisense	GGTGGGTCRTTCTTGCTGTC
Primer sets for qPCR		
CFTR	Sense	GGCTCTCACCTCAGAGATCG
	Antisense	ATGGCAGACACAATGACCAA
NKCC1a	Sense	GTGGTCAAGTTTGGCTGGAT
	Antisense	CATGGCAACAATCAAACAGG
NHE3	Sense	ATCAATGCAAACATGGACGA
	Antisense	AAGGAGGATAAAGCCCGTGT
NCC2	Sense	GGGCGTATTTCATGATCTCC
	Antisense	AATCCCGCATCATGTCAACG
EF1a	Sense	GAAGTTTGAGACCGGCAGG
	Antisense	CAACAATCAGCACAGCGCAG

Hybridoma Bank (DSHB), IA, USA] or a rabbit polyclonal antiserum raised against a synthetic peptide corresponding to part of the highly conserved region of the NKA α-subunit (NAK121; Uchida et al., 2000). The α5 antibody is a mouse monoclonal antibody against the avian NKA α-subunit and has been widely used to detect branchial NKA. The specificity of the antibody NAK121 was determined by Uchida et al. (2000). The antibody for NHE3 (Hiroi and McCormick, 2012) was raised against a mixture of two peptides corresponding to two different regions of rainbow trout (*Oncorhynchus mykiss*) NHE3b (GenBank accession number FJ376630); these regions are highly conserved among teleost NHE3 sequences, but are distinct from corresponding NHE2 sequences. Branchial CFTR was detected with a mouse monoclonal antibody against human CFTR (MAB25031, R&D Systems, Minneapolis, MN, USA). To detect NKCC1a and NCC2, we employed a mouse monoclonal T4 antibody (developed by Christian Lytle and Biff Forbush, and obtained from DSHB). While T4 antibody was directed against 310 amino acids at the C-terminus of human colonic NKCC1, the T4 antibody has been shown to react with both NKCC1a in the basolateral membrane and NCC2 in the apical membrane of ionocytes in tilapia and medaka (Hiroi and McCormick, 2012; Hsu et al., 2014).

Quadruple-color whole-mount immunofluorescence staining

The fixed gill filaments were washed in 0.01 mol l^{-1} phosphate-buffered saline containing 0.2% Triton X-100 (PBST) for 1 h, and treated with Image-iT FX signal enhancer (Thermo Fisher Scientific). The gill filaments were then incubated with a mixture of anti-NHE3, T4 and anti-CFTR antibodies for 2 days at 10°C. All antibodies were diluted with PBST containing 10% normal goat serum, 0.1% bovine serum albumin, 0.02% keyhole limpet hemocyanin and 0.01% sodium azide (NB-PBS) to a final dilution of 1:500. The samples were then incubated for 2 days at 10°C with a mixture of goat anti-rabbit IgG labeled with Alexa Fluor 488, goat anti-mouse IgG1 labeled with Alexa Fluor 555, and goat anti-mouse IgG2a labeled with Alexa Fluor 647 (Thermo Fisher Scientific), all diluted 1:500 with PBST. The filaments were washed in PBST, and subjected to post-staining fixation with 4% PFA in PB for 15 min. After washing in PBST, samples were incubated for 2 days at 10°C with α5 antibody directly labeled with Pacific blue using Zenon antibody labeling kit (Thermo Fisher Scientific) diluted 1:100 with NB-PBS. The gill filaments were washed in PBST, subjected to post-staining fixation with 4% PFA in PB for 15 min, washed briefly in PBST, and coverslipped with Prolong Gold Antifade Reagent (Thermo Fisher Scientific). The samples were observed with a Carl Zeiss LSM510 confocal laser scanning microscope (Zeiss, Jena, Germany). The wavelengths of excitation and recorded emission for each dye were as follows: Pacific Blue, 405 nm and >420 nm; Alexa Fluor 488, 488 nm and 505–530 nm; Alexa Fluor 555, 543 nm and 560–615 nm; and Alexa Fluor 647, 633 nm and >650 nm.

Triple-color whole-mount immunofluorescence staining and subsequent freeze sectioning

Gill filaments were removed from the gills fixed in 4% PFA in PB, washed in PBST for 1 h, and treated with Image-iT FX signal enhancer. The gill filaments were then incubated with a mixture of anti-NHE3 and T4 antibodies for 2 days at 4°C. Both antibodies were diluted 1:500 with NB-PBS. The samples were then incubated for 2 days at 4°C with a mixture of goat anti-rabbit IgG labeled with Alexa Fluor 555 and goat anti-mouse IgG labeled with Alexa Fluor 405 (Thermo Fisher Scientific), both diluted 1:500 with NB-PBS. The

filaments were then washed in PBST, and subjected to post-staining fixation with 4% PFA in PB for 15 min. After washing in PBST, the samples were incubated with fluorescein isothiocyanate (FITC)-labeled anti-NKA (Uchida et al., 2000) diluted 1:500 with NB-PBS for 3 days at 4°C. The stained gill filaments were rinsed in PBS, placed in PBS containing 30% sucrose, and then frozen in Tissue-Tek OCT Compound (Sakura Finetek, Tokyo, Japan). Cryosections (30 μm thick) were cut along the sagittal filamental axis in a cryostat at −20°C, and mounted on glass slides (Frontier, Matsunami Glass, Osaka, Japan). The samples were observed with a confocal laser scanning microscope (C1, Nikon, Tokyo, Japan). The wavelengths of excitation and recorded emission for each Alexa dye were as follows: Alexa Fluor 555, 543 nm and 568–643 nm; FITC, 488 nm and 500–530 nm; Alexa Fluor 405, 405 nm and 433–468 nm.

For quantitative analysis, NHE3/NKCC1a- or NCC2-immunoreactive ionocytes on the gill filaments and lamellae were separately counted on sagittal sections. According to the method described by Hirai et al. (1999), NKA-immunoreactive cells were classified into lamellar ionocytes when more than 50% of the sectional area appeared on a lamella, and into filament ionocytes in other cases. Previous studies have demonstrated that ionocytes in the filament were more abundant on the afferent vascular side than on the efferent (Cioni et al., 1991; Uchida et al., 1996; van der Heijden et al., 1997; Katoh et al., 2001; Sakamoto et al., 2001; Christensen et al., 2012). To overcome the uneven distribution of ionocytes in the gills, we randomly selected two sagittal sections cut through the afferent and efferent halves of the gill filaments from six individuals for each time point. The afferent sections are characterized by filaments with cartilage tissue appearing in the middle and short lamellae, while the efferent sections show full length of the lamellae. The number of ionocytes were counted along four lamellae and interlamellar regions, and expressed as the cell number per 1 mm of gill filament.

Detection of proliferating cells in the gills

For immunocytochemical detection of proliferating cells in the gills, we used a mouse monoclonal antibody against proliferating cell nuclear antigen (anti-PCNA, NA03, Calbiochem, Darmstadt, Germany). The fixed gills were washed in PBST for 1 h, and incubated overnight at 4°C with a mixture of anti-NKA (Uchida et al., 2000) and anti-PCNA diluted 1:1000 and 1:4000, respectively, with NB-PBS. After washing in PBST, the samples were then incubated overnight at 4°C with a mixture of goat anti-rabbit IgG labeled with Alexa Fluor 405 and goat anti-mouse IgG labeled with Alexa Fluor 488 (Thermo Fisher Scientific), both diluted 1:500 with NB-PBS. The stained gill filaments were rinsed in PBS, placed in PBS containing 30% sucrose, and then frozen in Tissue-Tek OCT Compound. Cryosections (10 μm thick) were cut along the sagittal filamental axis in a cryostat at −20°C, and mounted on glass slides (Frontier, Matsunami Glass). The samples were observed with the confocal laser scanning microscope (C1, Nikon).
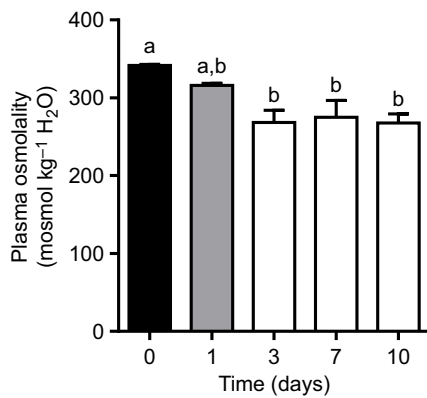
Statistics

All data were expressed as means±s.e.m. The significance of differences at $P<0.05$ was examined by the Kruskal–Wallis test followed by Dunn's test (Prism, version 6, GraphPad, San Diego, CA, USA).

RESULTS

Plasma osmolality

Mean plasma osmolality of fish maintained in SW (day 0) was 342 mosmol kg^{-1} H$_2$O. Plasma osmolality was significantly

Fig. 1. Changes in plasma osmolality after freshwater transfer in Japanese seabass. Time course change in plasma osmolality of fish transferred from seawater (day 0) to 10%-diluted seawater (day 1) and then to freshwater (days 3–10). Data are expressed as means±s.e.m. (N=6). Different letters indicate significant differences at $P<0.05$ (Dunn's test).

decreased but stayed within a narrow range from 268 to 295 mosmol kg^{-1} H$_2$O at 3, 7 and 10 days after the transfer (Fig. 1).

cDNA cloning of CFTR, NHE3, NKCC1a, NCC1, NCC2 and EF1a

To examine the ionocyte function of Japanese seabass in FW and SW, we first identified partial-length Japanese seabass CFTR (622 bp) and NHE3 (1039 bp) cDNAs, which encoded 207 and 346 amino acid residues, respectively. The deduced amino acid sequence of Japanese seabass CFTR showed 94% identity to killifish *Fundulus heteroclitus* CFTR (NP_001296904), 79% to zebrafish *Danio rerio* (NP_001038348), and 54% to mouse (NP_066388). The homology of the deduced amino acid

sequence of Japanese seabass NHE3 was 84, 83 and 66% to tilapia (AB326212), rainbow trout *Oncorhynchus mykiss* (FJ376630) and human NHE3 (BC101671), respectively. Sequenced NKCC1a was 622 bp in length and encoded 207 amino acid residues. The deduced amino acid sequence of Japanese seabass NKCC1a showed 95% identity to tilapia NKCC1a (AY513737), 93% to European eel *Anguilla anguilla* (AJ486858) and 83% to human (U30246), while it shared lower identities with NKCC1b of tilapia (85%, AY513738) and eel (87%, AJ486859). An isolated EF1a fragment of 815 bp encoded 271 amino acid residues. The homology of the deduced amino acid sequence of Japanese seabass EF1a showed 93% identity to medaka EF1a (NP_001098132) and 88% to human EF1a (EF362804). Accession numbers of Japanese seabass CFTR, NHE3, NKCC1a and EF1a were LC310873, LC310874, LC310875 and LC310876, respectively.

Secondly, we obtained partial cDNAs encoding two isoforms of NCC. An isolated NCC1 fragment was 1120 bp in length and encoded 373 amino acid residues. The deduced amino acid sequence of seabass NCC1 showed 83% identity to zebrafish NCC1 (BC155803) and 86% to medaka NCC1 (AB854642), and shared lower identities with NCC2 of zebrafish (60%, slc12a10.2, EF591989) and medaka (63%, slc12a10b, KJ489429). An NCC2 fragment of 1303 bp encoded 434 amino acid residues. The deduced amino acid sequence of seabass NCC2 showed 65 and 64% identity to zebrafish NCC1 and NCC2, respectively, and 63 and 70% to medaka NCC1 and NCC2, respectively. Reverse-transcription PCR analysis of NCC1 and NCC2 exhibited different expression patterns in different osmoregulatory organs. Whereas NCC1 was detected specifically in the kidney, NCC2 was primarily expressed in the gills in FW-acclimated fish (Fig. 2D). Accession numbers of Japanese seabass NCC1 and NCC2 were LC310877 and LC310878, respectively.
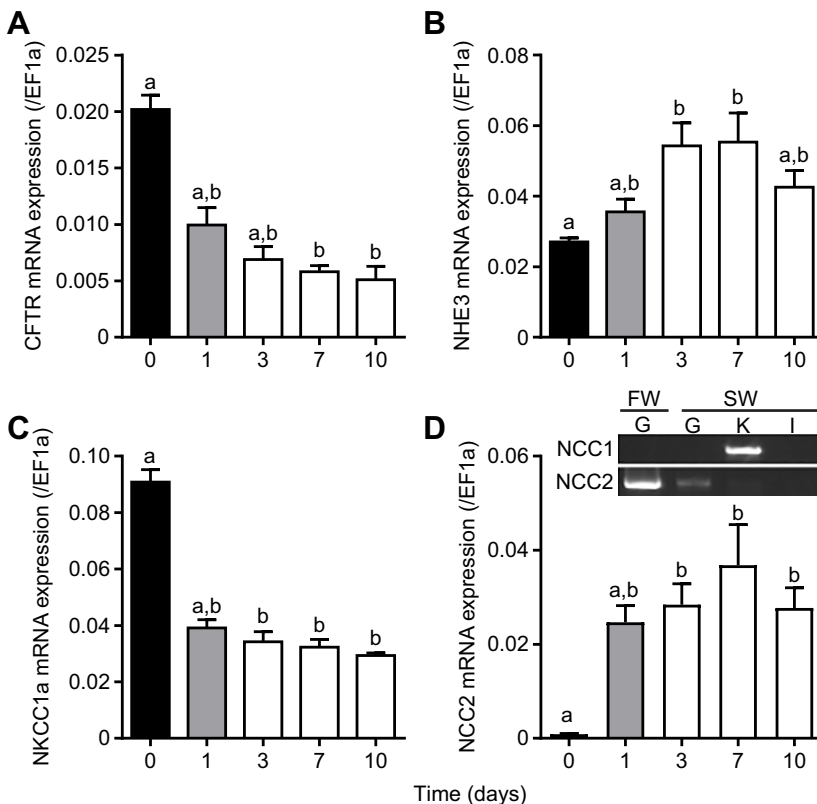
Fig. 2. Branchial gene expression of ion transporters. Changes in branchial gene expressions of cystic fibrosis transmembrane conductance regulator (CFTR, shown in A), Na$^+$/H$^+$ exchanger 3 (NHE3, shown in B), Na$^+$/K$^+$/2Cl$^-$ cotransporter 1a (NKCC1a, shown in C), and Na$^+$/Cl$^-$ cotransporter 2 (NCC2, shown in D) after transfer of Japanese seabass from seawater (day 0) to 10%-diluted seawater (day 1) and then to freshwater (days 3–10). Data are expressed as means±s.e.m. (N=6). Different letters indicate significant differences at $P<0.05$ (Dunn's test). (D) RT-PCR analysis of NCC1 and NCC2 in the osmoregulatory tissues. FW, freshwater; SW, seawater; G, gill; K, kidney; I, intestine.
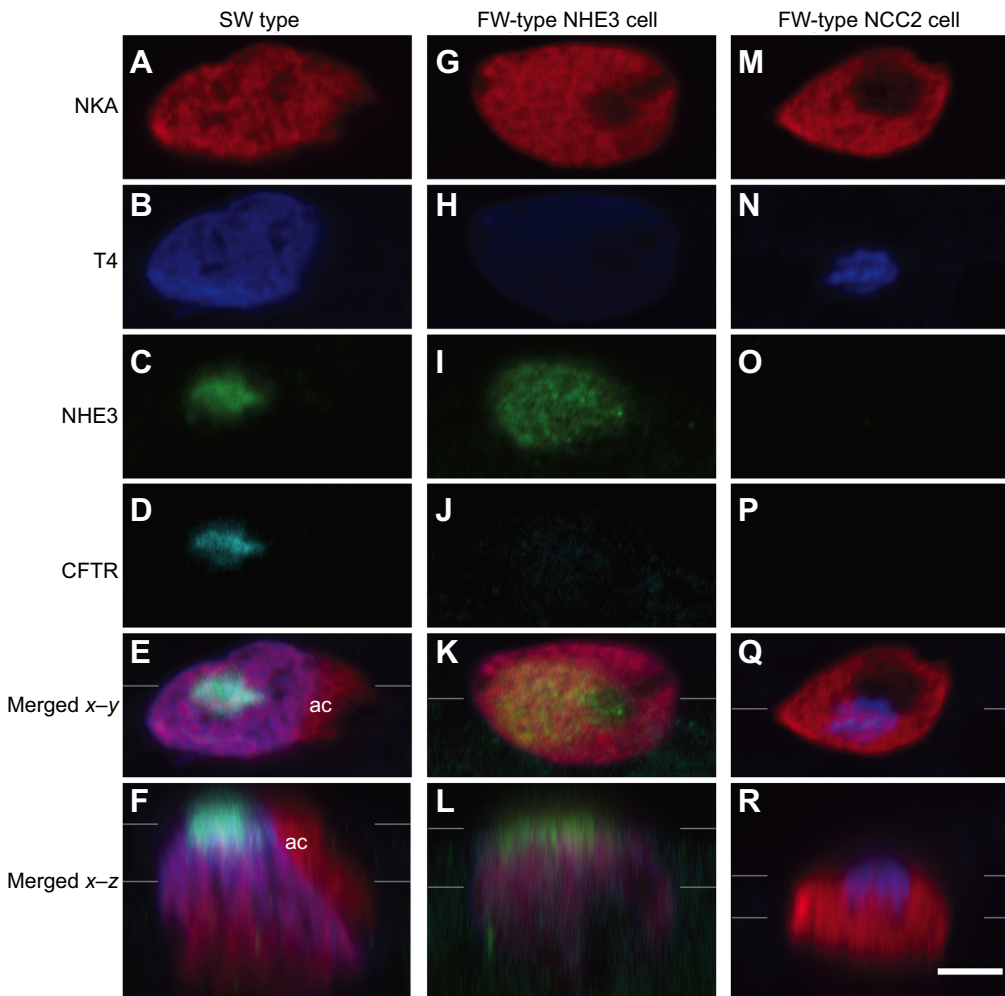
Fig. 3. Three different types of gill ionocytes in Japanese seabass. Quadruple immunofluorescence staining with anti-NKA (A,G,M; red), T4 (B,H,N; blue), anti-NHE3 (C,I,O; green) and anti-CFTR (D,J,P; cyan). (E,K,Q) Merged x–y images. (F,L,R) Merged x–z images. Merged x–y image: apical and basolateral signals of the x–y optical section cut at the upper and lower lines, respectively, indicated in merged x–z image; merged x–z image: the x–z optical section cut transversely at the horizontal lines indicated in merged x–y image. ac, accessory cell. Scale bar, 5 μm.

## Real-time quantitative polymerase chain reaction

We tested the branchial transcriptional responses during acclimation to the hypoosmotic environment. CFTR and NKCC1a mRNA expression were significantly decreased at 7 and 10 days after the transfer. The expression levels of CFTR were decreased to 49% at day 1 (1 day after 10% SW transfer), and to 25% at day 10 (Fig. 2A). Similar to the CFTR expression pattern, NKCC1a expression was decreased to 43% at day 1, and then the low levels (32–37%) were maintained until day 10 (Fig. 2C). By contrast, NHE3 and NCC2 expression levels were upregulated by the hypoosmotic challenge. The expression of NHE3 was significantly increased 2-fold at days 3 and 7 compared with the SW control; however, the NHE3 expression was decreased at day 10 to a level that was not significantly different from the value at day 0 (Fig. 2B). NCC2 mRNA levels were markedly increased after transfer. The expression levels of NCC2 were 28- to 42-fold higher at days 1 to 10 than at day 0 (Fig. 2D).

Quadruple-color whole-mount immunofluorescence staining

The immunoreactions with anti-NHE3, anti-CFTR and T4 antibodies were restricted to NKA-immunoreactive ionocytes, but not detected in the other cell types in the gill epithelium. In agreement with previous studies (Hiroi and McCormick, 2012; Hsu et al., 2014), T4 signals were observed in the basolateral region of SW-type ionocytes (Fig. 3B) and in the apical region of FW-type ionocytes (Fig. 3N). Most probably, these T4 signals can be attributed to NKCC1a when it appears in the basolateral side and to NCC2 when it is in the apical side in Japanese seabass, as well as in other teleosts examined. Based on distribution patterns of NHE3, CFTR and T4 signals, Japanese seabass ionocytes were largely classified into the following three types: (1) ionocytes with apical CFTR and NHE3 and basolateral NKCC1a (SW type; Fig. 3A–F); (2) ionocytes with apical NHE3 (FW-type NHE3 cell; Fig. 3G–L); and (3) ionocytes with apical NCC2 (FW-type NCC2 cell; Fig. 3M–R). The SW-type ionocytes typically formed multicellular complexes with distinct accessory cells. Although main cells showed NKA and NKCC1a immunosignals, the accessory cells showed only NKA immunoreaction in the basolateral membrane (Fig. 3E,F). Basolateral NKCC1a immunoreactivity was also detected in FW-type NHE3 cells, but the immunosignals were much weaker in FW-type NHE3 ionocytes than in SW-type cells (Fig. 3B,H).

The SW-type ionocytes occupied the greatest proportion of ionocyte population in the gill epithelia of Japanese seabass at days 0 and 1 of transfer (Fig. 4A–J). Following transfer to hypoosmotic water, CFTR immunosignals disappeared by day 3 (Fig. 4D,I,N,S,X). Although basolateral NKCC1a faded by day 7, apical NCC2 signals appeared at day 3 and were increased at day 10 after transfer (Fig. 4B,G,L,Q,V). However, NHE3 signals were constantly detected during the transfer experiment (Fig. 4C,H,M,R,W). In fish acclimated to FW at the end of transfer experiment (day 10), ionocytes consisted
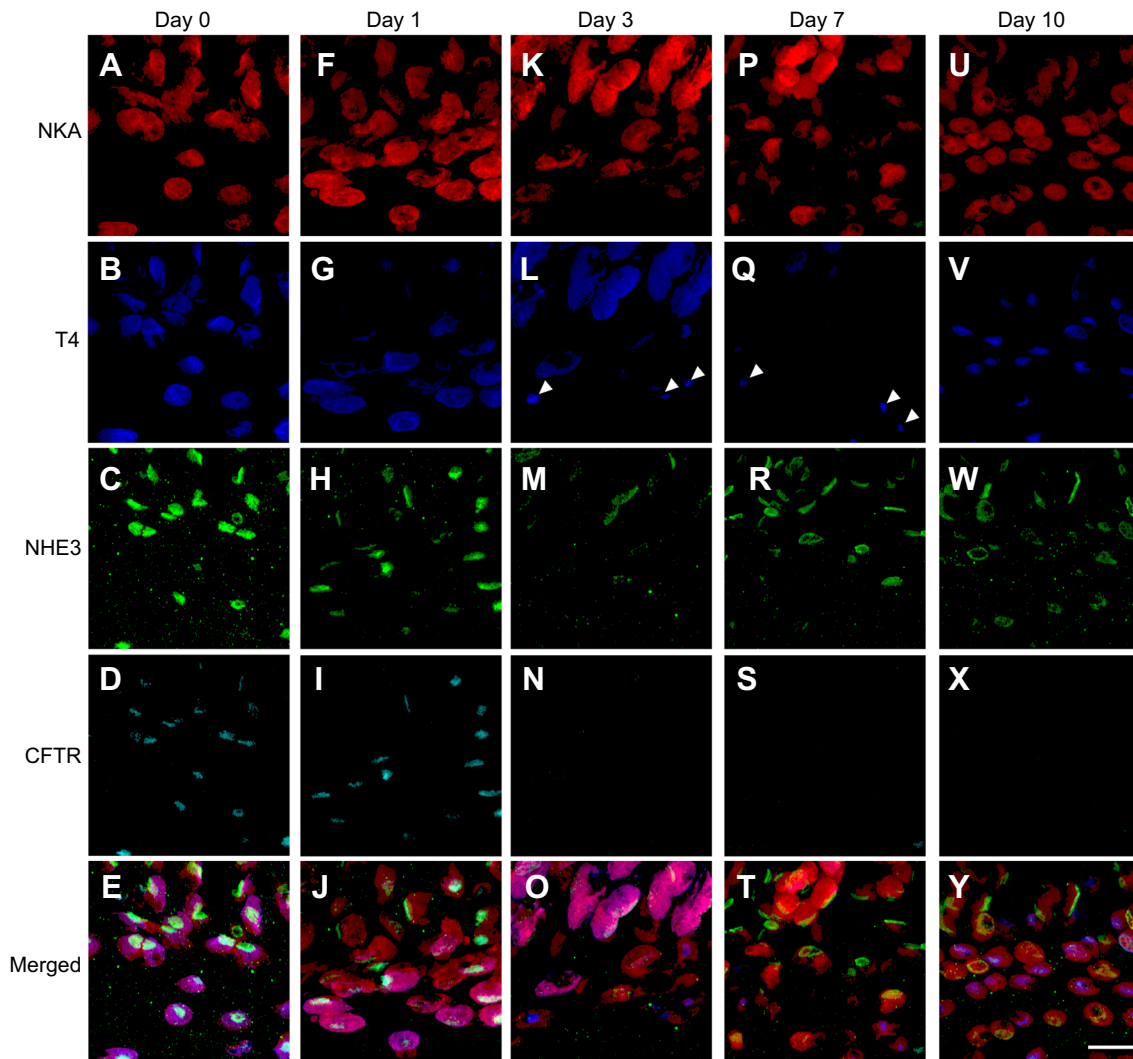
Fig. 4. Whole-mount immunostaining with anti-NKA, T4, anti-NHE3 and anti-CFTR in the gills. Quadruple immunofluorescence staining with anti-NKA (A,F,K,P,U; red), T4 (B,G,L,Q,V; blue), anti-NHE3 (C,H,M,R,W; green) and anti-CFTR (D,I,N,S,X; cyan) in the gills of Japanese seabass at days 0 (A–E), 1 (F–J), 3 (K–O), 7 (P–T) and 10 (U–Y) after transfer from seawater to freshwater. The afferent side of filaments is horizontal in the lower half of each image, and lamellae are seen perpendicular to each filament. (E,J,O,T,Y) Merged images. Arrowheads indicate apical T4 signals at days 3 and 7. Scale bar, 20 μm.

mostly of FW-type NHE3 cells and FW-type NCC2 cells (Fig. 4U–Y).

The cross-sectional images of ionocytes revealed the difference in shape of NHE3-immunoreactive apical regions between SW-type and FW-type NHE3 ionocytes (Fig. 5). In SW-type ionocytes, NHE3 signals were colocalized with CFTR in the apical region, which often showed a U-shaped appearance (Fig. 5C,D). However, FW-type NHE3 ionocytes showed only NHE3 immunoreaction but lacked CFTR in the apical area, which had a convex appearance (Fig. 5M,N). In addition to these two types of ionocytes, some cells with apical NHE3 had intermediate features between SW-type and FW-type NHE3 ionocytes (Fig. 5F–J). These cells were frequently observed at day 1, but rarely seen at the other time points of transfer. The intermediate-type ionocytes were characterized by colocalization of CFTR and NHE3 in the convex apical membrane (Fig. 5H,I). The immunoreaction with T4 antibody was observed in the basolateral region of both SW-type and intermediate-type cells (Fig. 5B,G,L).

Distributional changes of gill ionocytes during transfer from SW to FW

We examined the distributional change of ionocytes on cryosections of gill filaments stained with anti-NKA, anti-NHE3 and T4 antibodies (Fig. 6). In SW-acclimated fish (day 0), the distribution of ionocytes was restricted to the filament epithelia, and ionocytes were not observed in the gill lamellae. Those ionocytes in the filaments showed apical NHE3 and basolateral NKA and NKCC1a immunoreactions (Fig. 6A–D). At 10 days after transfer to FW, however, ionocytes were detected in both filaments and lamellae. Although most lamellar ionocytes showed NHE3 and/or NKCC1a, filament ionocytes were characterized by apical NCC2 immunoreaction (Fig. 6E–H).

For quantitative analyses, the density of ionocytes was measured separately in the gill filaments and lamellae (Fig. 7). Although the total number of NKA-immunoreactive ionocytes in filaments was not significantly different, the ionocyte density in the lamellae was significantly increased at day 10 after transfer to hypoosmotic water, compared with day 0 (SW control) and day 1 (Fig. 7A,B). The
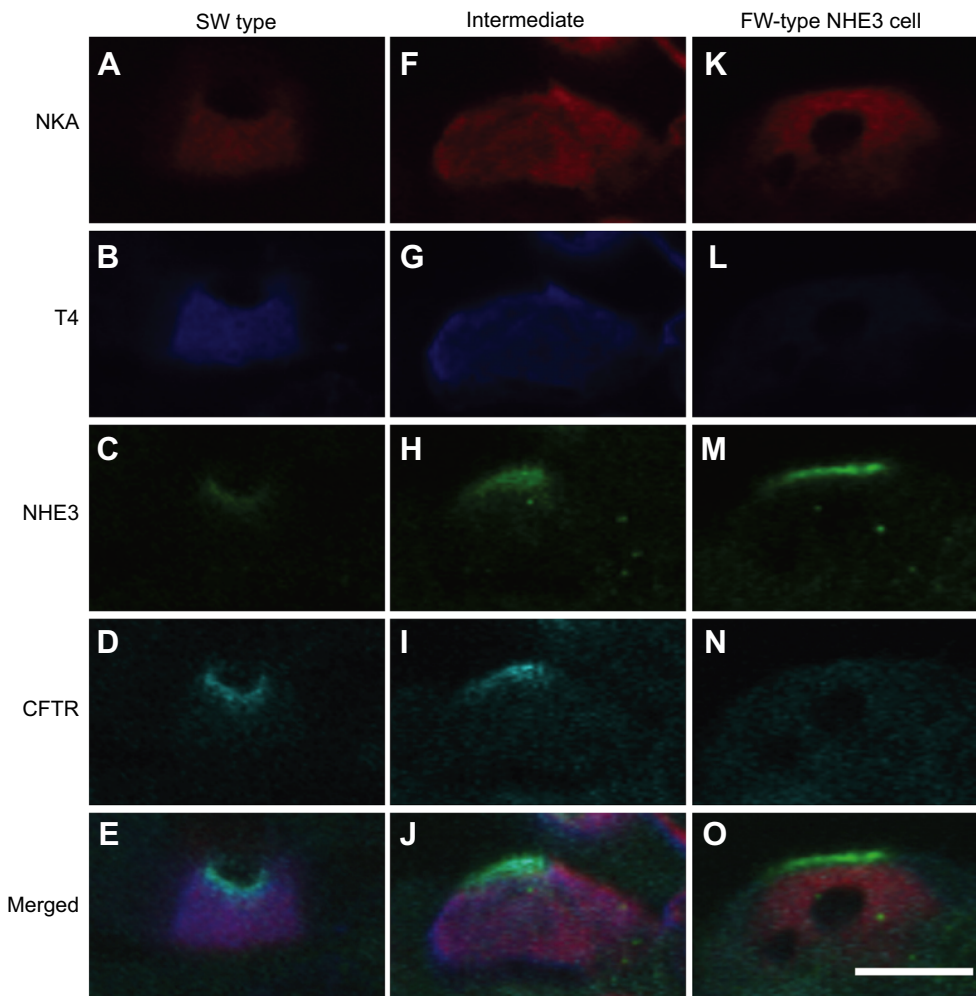
Fig. 5. The intermediate type of gill ionocytes. x–z images of a SW-type ionocyte (A–E), a FW-type NHE3 ionocyte (K–O) and the intermediate-type cell (F–J) in the gills of Japanese seabass, immunostained with anti-NKA (A,F,K; red), T4 (B,G,L; blue), anti-NHE3 (C,H,M; green) and anti-CFTR (D,I,N; cyan). (E,J,O) Merged images. Scale bar, 10 µm.

density of NHE3/NKCC1a ionocytes in filaments gradually decreased from day 0 to day 3 after the transfer, and the density was significantly lower at day 10 than day 0 (Fig. 7C). In contrast, NHE3/NKCC1a ionocytes were not detected in lamellae at day 0, and then increased markedly at day 10 (Fig. 7D). The NHE3/NKCC1a ionocytes include three types of ionocytes: ionocytes with apical NHE3 and basolateral NKCC1a, accounting for 74–91% of NHE3/NKCC1a ionocytes throughout the experiment period; those with only basolateral NKCC1a (9–20%); and those with only apical NHE3 (2–10%). Although NCC2 ionocytes were absent from the gill filaments in SW at day 0, NCC2 cells appeared in the filaments on transfer to hypoosmotic water and were significantly increased at days 7 and 10 compared with day 0 (Fig. 7E). Meanwhile, NCC2 ionocytes were rarely found in the lamellar epithelia during the transfer experiment (Fig. 7F). Although few in number, ionocytes with apical NHE3 and NCC2 (1.1% of the total number of ionocytes) were observed in filaments at day 7 and in lamellae at days 7 and 10.

### Distribution of proliferating cells in the gills
For the examination of ionocyte progenitors in the gills, ionocytes and proliferating cells were detected simultaneously by double immunofluorescence staining for NKA and PCNA. Although NKA-immunoreactive ionocytes shifted their distribution from filaments to lamellae after transfer from SW to FW, PCNA-immunoreactive nuclei were detected mainly in the gill filaments

and rarely in the lamellae through the experimental period of 10 days (Fig. 8).

DISCUSSION
In the present study, we characterized one SW-type, two FW-type and an intermediate-type ionocyte in Japanese seabass. On the basis of this classification, we explored the distributional change of Japanese seabass ionocytes in the gill filament and lamellar epithelia. Although plasma osmolality was significantly decreased following transfer from SW to FW, those levels were maintained within a physiological range throughout the experimental period, indicating their successful acclimation to FW.

In our molecular analysis, we identified partial cDNAs encoding CFTR, NHE3, NKCC1a, NCC1, NCC2 and EF1a. Our sequence analyses showed the high homology of these sequences between Japanese seabass and other vertebrates. In previous studies, phylogenetic analyses have revealed that NCC-like cotransporters of vertebrates are clearly divided into two clades, namely, the conventional NCC clade and fish-specific NCC clade (Hiroi and McCormick, 2012; Takei et al., 2014). Although the well-known NCC such as human NCC and winter flounder NCC were assigned to the conventional NCC (slc12a3 or NCC1) clade, the fish-specific NCC (slc12a10 or NCC2) was initially identified in tilapia (Hiroi et al., 2008) and subsequently in zebrafish and medaka (Wang et al., 2009; Hsu et al., 2014). The NCC1 is restricted to renal tissues in teleosts, but the NCC2 is expressed in extrarenal tissues such as the
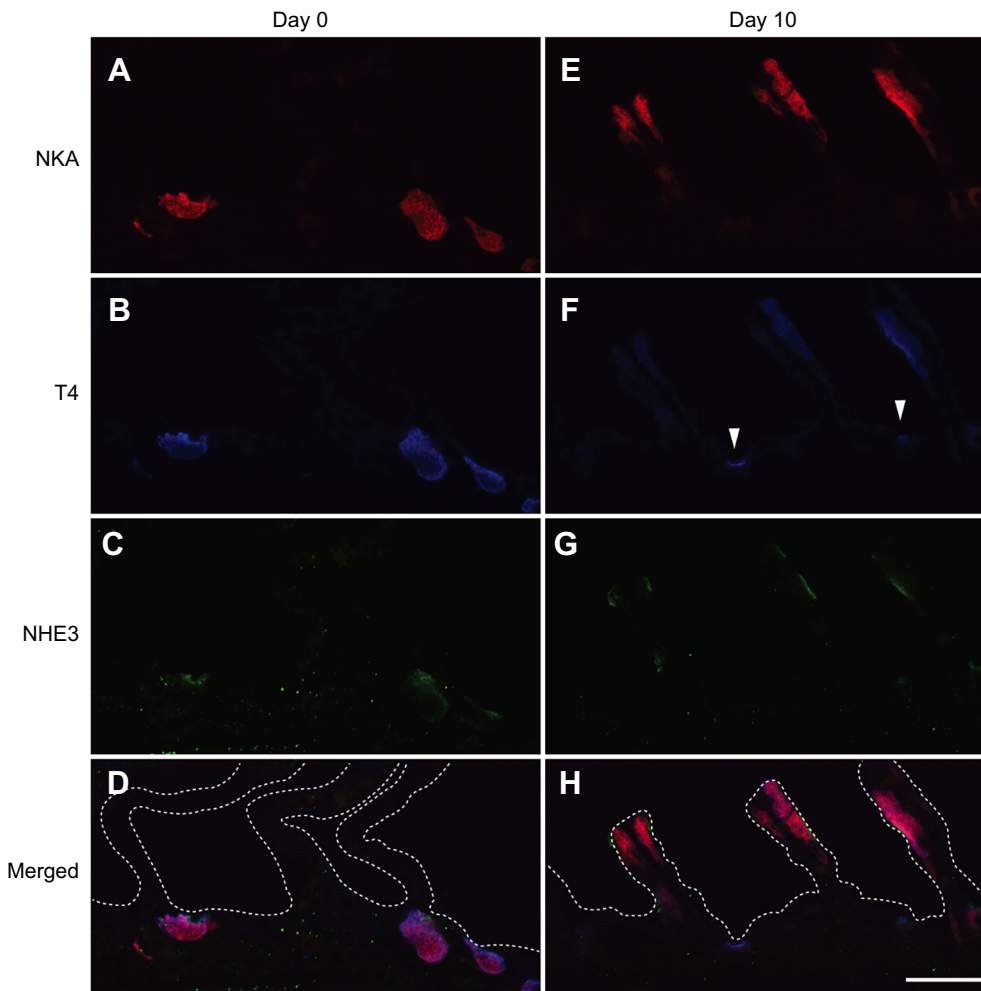
Fig. 6. Immunostaining with anti-NKA, T4 and anti-NHE3 in frozen section of the gills. Ionocytes on the cryosections of the gill filaments subjected to triple-color immunofluorescence staining with anti-NKA (A,E; red), T4 (B,F; blue) and anti-NHE3 (C,G; green) in the gills of Japanese seabass at day 0 (A–D) and day 10 (E–H) after transfer from seawater to freshwater. (D,H) Merged images. Arrowheads indicate apical T4 signals. Scale bar, 20 μm.

gills and intestine (Hiroi et al., 2008; Wang et al., 2009; Kato et al., 2011; Teranishi et al., 2013; Hsu et al., 2014). We also characterized two isoforms of NCC in Japanese seabass. Consistent with previous reports, Japanese seabass NCC1 and NCC2 were expressed in the kidney and gills, respectively. Thus, in this study, we focused on NCC2 for further experiments on branchial ionocytes.

In order to investigate the branchial ionoregulatory mechanisms in Japanese seabass, we compared the gene expressions of CFTR, NHE3, NKCC1a and NCC2 in the gills following transfer from SW to FW. In agreement with the currently accepted model of ion secretion in SW ionocytes (Hwang and Lin, 2013; Marshall, 2013), the expression levels of CFTR and NKCC1a in the gills rapidly decreased after transfer to FW. Similar to our results, downregulation of CFTR and NKCC1a expression following hypoosmotic stimuli has also been reported in Mozambique tilapia (Hiroi et al., 2008; Moorman et al., 2014), killifish (Scott et al., 2005) and European seabass *Dicentrarchus labrax* (Lorin-Nebel et al., 2006; Bodinier et al., 2009). This result confirms that the proposed molecular mechanism of ion-secreting ionocytes is also applicable to Japanese seabass. In contrast, the mechanisms for ion uptake of FW ionocytes vary according to species (Hwang and Lin, 2013). In Mozambique tilapia, zebrafish, medaka and killifish, NKA, NCC2 and NHE3 are considered to be involved in Na^+ and Cl^- uptake in FW ionocytes (Hiroi et al., 2008; Inokuchi et al., 2008; Wang et al., 2009; Chang et al., 2013; Hsu et al., 2014). However, NCC2 does not seem to be expressed in the gills of salmonids and eels, whereas NHE3 was indicated to be involved in

ion uptake in FW ionocytes (Ivanis et al., 2008; Seo et al., 2013; Takei et al., 2014). In the present study, both NHE3 and NCC2 were upregulated in the gills of Japanese seabass following FW transfer, indicating that both NHE3 and NCC2 were importantly involved in ion uptake.

We applied simultaneous immunofluorescence staining with anti-NKA, anti-NHE3, anti-CFTR and T4 antibodies to the gills to make a functional classification of Japanese seabass ionocytes. The T4 antibody can be used to detect both apical NCC2 and basolateral NKCC1a in ionocytes of Mozambique tilapia (Hiroi and McCormick, 2012) and medaka (Hsu et al., 2014). According to ion-transporting proteins expressed in the apical and basolateral membranes, we successfully classified NKA-immunoreactive ionocytes into three types. The first type is ionocytes with apical NHE3 and CFTR and basolateral NKCC1a, which predominate in the gills of SW-acclimated fish. We observed the other two types mostly in FW-acclimated fish; that is, ionocytes with apical NHE3 (FW-type NHE3 cell), and those with apical NCC2 (FW-type NCC2 cell). The ionocyte classification of Japanese seabass is very similar to that proposed in Mozambique tilapia, which belongs to the same Perciformes order as Japanese seabass (Hiroi et al., 2008; Inokuchi et al., 2008). The SW-type ionocyte, FW-type NHE3 cell and FW-type NCC2 cell are equivalent to type IV, type III and type II, respectively, in Mozambique tilapia (Hiroi et al., 2005, 2008). In contrast to SW ionocytes, the mechanisms for ion uptake in ionocytes of FW-acclimated teleosts vary among species. For example, as well as in Japanese seabass and Mozambique tilapia,
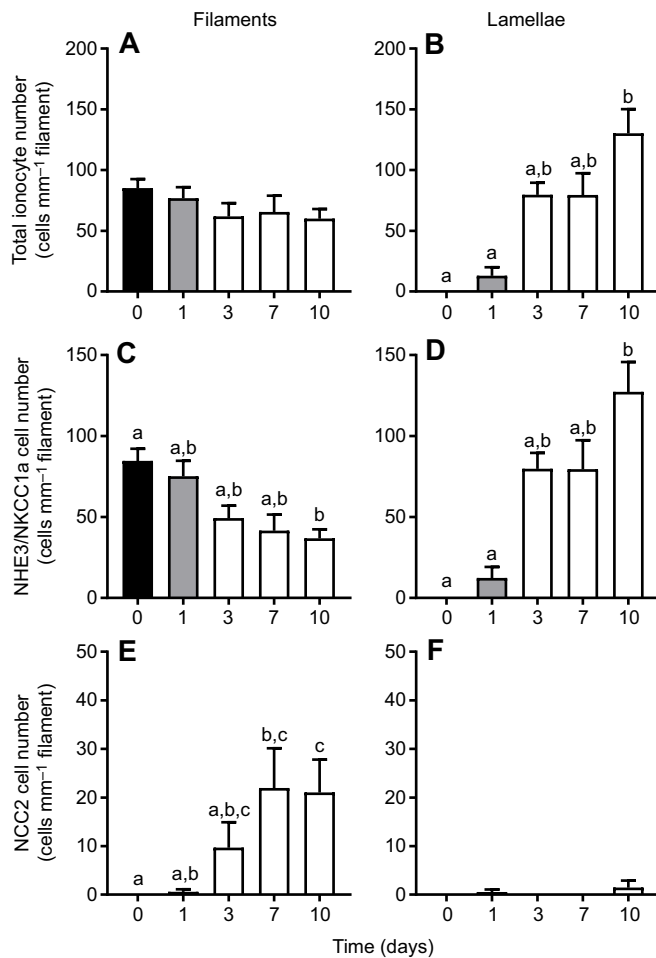
Fig. 7. Distributional changes of gill ionocytes. Changes in the numbers of all ionocytes (A,B), NHE3/NKCC1a ionocytes (C,D) and NCC2 ionocytes (E,F) in gill filaments (A,C,E) and lamellae (B,D,F) of Japanese seabass transferred from seawater (day 0) to 10%-diluted seawater (day 1) and then to freshwater (days 3–7). Data are expressed as means±s.e.m. (N=6). Different letters indicate significant differences at $P<0.05$ (Dunn's test).

NHE3 cells and NCC2 cells were also identified in the gills of FW medaka (Hsu et al., 2014). These three species belong to the superorder Acanthopterygii. However, NCC2 cells were not found in the spotted green pufferfish, which also belongs to Acanthopterygii (Tang et al., 2011). However, NCC2 cells have not been observed in the gills of eels and salmonids, belonging to more primitive teleost taxa, superorders Elopomorpha and Protacanthopterygii, respectively (Pelis et al., 2001; Tipsmark et al., 2002; Wilson et al., 2004; Hiroi and McCormick, 2007; Seo et al., 2013). In superorder Ostariophysi, NCC2 cells were detected in zebrafish, but not in milkfish (Wang et al., 2009; Tang et al., 2011). As it is difficult to analyse the evolutionary trends in ionocyte classification so far, more immunocytochemical evidence for other species is required for further investigation.

Although most FW-type ionocytes appear as single cells, SW-type ionocytes frequently form multicellular complexes. In Japanese seabass, the complexes usually consist of a NKA- and NKCC1a-immunoreactive main cell and a NKA-immunoreactive small cell. Because the small cell is located on the shoulder of the main cell and these two cells seem to share a common apical pit, the small cell is considered as an accessory cell. It has been proposed that the apical junctions between main ionocytes and accessory cells

form a leaky paracellular route for Na⁺ excretion in SW (Sardet et al., 1979; Hootman and Philpott, 1980; Hwang and Hirano, 1985; Shen et al., 2011). In addition, it has been controversial whether the accessory cell is a discrete cell type (Pisam et al., 2000) or merely an early developmental stage of ionocytes (Wendelaar Bonga and van derMeij, 1989; Wendelaar Bonga et al., 1990; Inokuchi and Kaneko, 2012). As accessory cells can be distinguished from main cells by the absence of NKCC1a signals, Japanese seabass might be useful for investigating the role of accessory cells in fish osmoregulation.

The immunoreactivity of CFTR was completely extinguished at day 3 after transfer from SW to FW, indicating that SW-type ionocytes disappeared and, in turn, FW-type NHE3 cells appeared within 3 days after transfer. However, FW-type NCC2 ionocytes were absent in SW, appeared at day 3 after transfer, and increased in number thereafter. As apical NCC2 in FW ionocytes is specific for FW and considered as a pathway to absorb Na⁺ and Cl⁻, the increasing trend of this type is regarded as an adaptive response to the hypoosmotic environment (Hiroi et al., 2008; Inokuchi et al., 2008, 2009; Horng et al., 2009; Wang et al., 2009). We simultaneously observed disappearance of SW-type cells and appearance of NCC2 cells at day 3, implying that the shift of the osmoregulatory mechanism from FW to SW acclimation was completed within 3 days after transfer.

The immunoreactivity of NHE3 was consistently observed in ionocytes throughout the experimental period. Previous studies reported that NHE3 plays a role in the Na⁺ uptake mechanism of FW ionocytes in tilapia, zebrafish and medaka (Esaki et al., 2007; Yan et al., 2007; Lin et al., 2008; Inokuchi et al., 2009; Wu et al., 2010; Kumai and Perry, 2011); however, our results showed that NHE3 immunoreaction was also detected in SW fish. In Atlantic stingray *Dasyatis sabina* (Choe et al., 2005), killifish (Claiborne et al., 1999; Edwards et al., 2005), tilapia (Watanabe et al., 2008), rainbow trout (Edwards et al., 1999; Ivanis et al., 2008) and Japanese eel *Anguilla japonica* (Seo et al., 2013), apical NHE3 immunoreaction was detected not only in FW-type ionocytes but also in SW ionocytes. In SW fish, NHE in the apical membrane of ionocytes is thought to be the major transporter for acid secretion (Claiborne et al., 2002). In medaka gills, mRNA levels of NHE2 and NHE3 were upregulated by acidified SW (pH 7), suggesting that NHE was involved in acid secretion by SW-type ionocytes (Liu et al., 2016). Moreover, applying the scanning ion-selective electrode technique (SIET), Liu et al. (2013, 2016) have shown that treatment with an inhibitor of NHE suppressed both H⁺ and Cl⁻ secretion at ionocytes of SW-acclimated medaka larvae. These findings indicate that NHE2 and NHE3 play critical roles in acid secretion, and that the acid secretion is linked to Cl⁻ secretion in SW.

Although CFTR immunoreaction disappeared within 3 days, that of NKCC1a, which coexpressed with CFTR in SW-type cells, remained even at day 3. One possible explanation for the disappearance of CFTR followed by NKCC1a is that SW-type ionocytes suppress CFTR and NKCC1a in series, and consequently transform into FW-type NHE3 ionocytes. Our immunocytochemical observation revealed the occurrence of intermediate-type ionocytes between SW-type and FW-type NHE3 cells at 1 day after transfer. The intermediate-type ionocytes showed apical CFTR and NHE3 immunoreactions, which are characteristic of SW-type cells; however, their apical region showing a convex appearance is more like FW-type NHE3 ionocytes. The intensity of NKCC1a immunoreaction was at the intermediate level between SW-type and FW-type NHE3 ionocytes. Considering that the intermediate-type cells transiently appeared at day 1 after transfer, it is most probable that
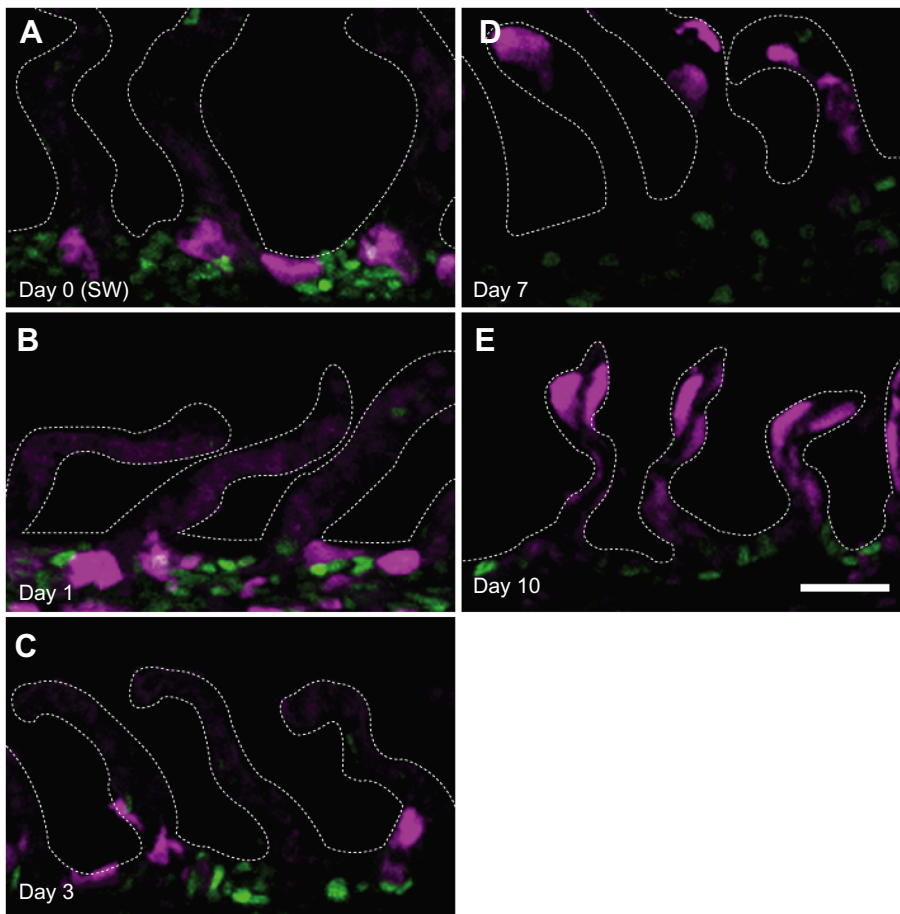
Fig. 8. Distribution of proliferating cells in the gills. Double immunofluorescence staining with anti-NKA (magenta) and anti-PCNA (green) in the gills of Japanese seabass at days 0 (A), 1 (B), 3 (C), 7 (D) and 10 (E) after transfer from seawater to freshwater. Scale bar, 20 μm.

SW-type ionocytes were transformed into FW-type NHE3 ionocytes via the intermediate type. In tilapia, following *in vivo* sequential changes of individual ionocytes, Hiroi et al. (1999) showed that 75% of the cells survived at 96 h after transfer from FW to SW, and that single FW-type ionocytes were transformed into multicellular SW-type ionocytes. Subsequent studies showed that decrease of FW-type NHE3 (type III) cells and increase of the SW-type (type IV) cells occurred within 24 h after transfer from FW to SW, suggesting that the type III cells directly transformed into the type IV cells in tilapia (Hiroi et al., 2005; Choi et al., 2011). Furthermore, using the SIET, Shen et al. (2011) demonstrated the functional change from ion uptake to ion secretion in individual ionocytes in the skin of medaka larvae during acute salinity change. Taken together, our immunocytochemical

observations are most likely to indicate functional plasticity of ionocytes.

As reported in Japanese seabass juveniles (Hirai et al., 1999), this study showed that all branchial ionocytes were detected in gill filaments in fish reared in SW, whereas lamellar ionocytes appeared in fish transferred to FW. To further examine the mechanisms of distributional change of ionocytes, we observed the location of ionocyte subtypes in the gill filaments and lamellae on cryosections of the gills. We adopted triple-color immunofluorescence staining with anti-NKA, anti-NHE3 and T4 antibodies before freeze-sectioning of the gill filaments. Considering that SW-type is probably transformed into FW-type NHE3 cells, we grouped these two types into the NHE3/NKCC1a cell type. Our immunocytochemical observation
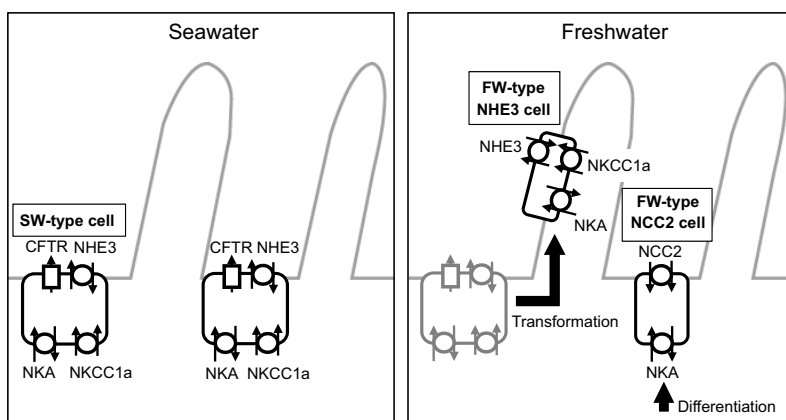
Fig. 9. Functional classification of gill ionocytes and spatiotemporal changes in their distribution. Schematic diagrams showing distributional changes of three distinct types of ionocytes in the gill filaments and lamellae of Japanese seabass transferred from seawater to freshwater.

showed differential distribution patterns of NCC2 ionocytes and NHE3/NKCC1a ionocytes in gill filaments and lamellae. The number of NHE3/NKCC1a ionocytes, which included FW-type NHE3 cells and SW-type cells, increased progressively in gill lamellae during FW acclimation, while their density gradually decreased in gill filaments. The apical region of NHE3/NKCC1a cells formed a small pit in SW, but became large and flat at 10 days after FW transfer. These results indicate that, following FW transfer, SW-type ionocytes altered their function and morphology to transform into FW-type NHE3 ionocytes, concomitantly with their distribution shift from gill filaments to lamellae.

Interestingly, NCC2 ionocytes that were absent in SW appeared after transfer to FW in the filaments, but were rarely observed in the lamellae through the transfer experiment. To our knowledge, this is the first effort to quantify the distributional change of NCC2 ionocytes following salinity change. Although different distribution patterns of ionocytes in the gills have been reported in teleost species, FW-type ionocytes are often present in the lamellae in FW but not in SW in several teleost species, e.g. chum salmon *Oncorhynchus keta* (Uchida et al., 1996), Japanese eel (Sasai et al., 1998), Japanese seabass (Hirai et al., 1999), European seabass (Varsamos et al., 2002), milkfish *Chanos chanos* (Lin et al., 2006) and alewife *Alosa pseudoharengus* (Christensen et al., 2012). These observations have led to the hypothesis that lamellar ionocytes are involved in ion uptake in FW and filament ionocytes are responsible for ion secretion in SW (Pisam et al., 1988; Uchida et al., 1996; Sasai et al., 1998; Hirai et al., 1999; Seidelin et al., 2000; Pelis et al., 2001; Zydlewski and McCormick, 2001). However, in our study, ion-absorptive NCC2 ionocytes were mainly observed in the gill filaments. Although NCC2 ionocytes were predominantly observed in the gill filaments after FW transfer, a small number of those cells appeared in the lamellae at day 10 after transfer. As NCC2 ionocytes were specifically observed in FW, they seemed to be newly differentiated after transfer from SW to FW. Taken together, it is likely that transfer from SW to FW induced NCC2-ionocyte differentiation in the gill filaments. Although most of the newly induced NCC2-ionocytes stay in the filaments, some cells seem to migrate to the lamellae during the experimental period of 10 days.

The mechanism of distributional change of gill ionocytes is still controversial. In the gills of chum salmon and tilapia, undifferentiated cells were mainly observed in the deeper layer of the filament epithelium (Uchida and Kaneko, 1996; Dang et al., 1999). Therefore, the lamellar ionocytes were considered to be recruited in the filaments and then migrated to the lamellae (Hirai et al., 1999). Recently, however, proliferating cells were observed not only in the filament epithelia but also in the lamellar epithelia in zebrafish and air-breathing fish *Trichogaster leeri*, suggesting that lamellar ionocytes can be locally differentiated from lamellar progenitor cells (Chou et al., 2008; Lee et al., 2008). We observed undifferentiated cells in the gills of Japanese seabass by means of PCNA immunocytochemistry. The undifferentiated cells were detected mainly in the gill filaments and rarely in the lamellae, and those undifferentiated cells in the lamellae were not increased during the experiment. Our findings indicate that transfer from SW to FW induces differentiation of NCC2 ionocytes in the gill filament epithelia. Those NCC2 ionocytes originating from undifferentiated cells in the filaments further expand their distribution to the lamellae during FW acclimation.

It is not clear why ionocytes are mostly observed in the filaments in SW and spread their distribution to lamellae during FW acclimation. In the present study, the total number of lamellar ionocytes was increased after FW transfer, but that of filament ionocytes did not change throughout the experimental period. This result suggests that FW acclimation of Japanese seabass requires the increase in ionocyte population to enhance ionoregulatory capacities. Because insufficient space was available in the filaments, ionocytes were forced to expand their distribution to the lamellae to compete with pavement cells for the surface area. When European seabass were acclimated to doubly concentrated SW, a rich population of ionocytes was found in the gill lamellae as well as in the filaments (Varsamos et al., 2002). Those lamellar ionocytes in this species are likely to be involved in active ion secretion in hypertonic environments, suggesting that increase in the number of ionocytes, rather than enhancement of FW adaptability, accounts for the appearance of lamellar ionocytes.

In the present study, spatiotemporal changes in branchial ionocyte distribution were investigated following transfer of Japanese seabass from SW to FW. The characteristics of different types of ionocytes and their distributional changes are summarized in Fig. 9. Our findings indicated that SW-type ionocytes transformed into FW-type NHE3 ionocytes and, at the same time, shifted their distribution from the gill filaments to lamellae. However, FW-specific NCC2 ionocytes appeared mainly in the filaments after FW transfer. The clear salinity-induced change in the distributional pattern of ionocytes in the gills was first observed in chum salmon (Uchida et al., 1996), and has been confirmed in a variety of teleosts. It took another two decades to clarify the mechanism of distributional changes of ionocytes. Our findings indicate that FW transfer promotes migration of ionocytes from the filaments to lamellae to enhance hyperosmoregulatory capacities. Under natural conditions, Japanese seabass juveniles change their habitat from SW to estuaries or rivers. The migration of ionocytes may contribute to their acute response to osmotic fluctuations and their tolerance to a wide range of salinities.

References
Bodinier, C., Boulo, V., Lorin-Nebel, C. and Charmantier, G. (2009). Influence of salinity on the localization and expression of the CFTR chloride channel in the ionocytes of *Dicentrarchus labrax* during ontogeny. *J. Anat.* **214**, 318-329.

Chang, W.-J., Wang, Y.-F., Hu, H.-J., Wang, J.-H., Lee, T.-H. and Hwang, P.-P. (2013). Compensatory regulation of Na$^+$ absorption by Na$^+$/H$^+$ exchanger and Na$^+$-Cl$^-$ cotransporter in zebrafish (*Danio rerio*). *Front. Zool.* **10**, 46.

Choe, K. P., Kato, A., Hirose, S., Plata, C., Sindic, A., Romero, M. F., Claiborne, J. B. and Evans, D. H. (2005). NHE3 in an ancestral vertebrate: primary sequence, distribution, localization, and function in gills. *Am. J. Physiol. Regul. Integr. Comp. Physiol.* **289**, R1520-R1534.

Choi, J. H., Lee, K. M., Inokuchi, M. and Kaneko, T. (2011). Morphofunctional modifications in gill mitochondria-rich cells of Mozambique tilapia transferred from freshwater to 70% seawater, detected by dual observations of whole-mount immunocytochemistry and scanning electron microscopy. *Comp. Biochem. Physiol. A* **158**, 132-142.

Chou, M.-Y., Hsiao, C.-D., Chen, S.-C., Chen, I.-W., Liu, S.-T. and Hwang, P.-P. (2008). Effects of hypothermia on gene expression in zebrafish gills: upregulation in differentiation and function of ionocytes as compensatory responses. *J. Exp. Biol.* **211**, 3077-3084.

Christensen, A. K., Hiroi, J., Schultz, E. T. and McCormick, S. D. (2012). Branchial ionocyte organization and ion-transport protein expression in juvenile alewives acclimated to freshwater or seawater. *J. Exp. Biol.* **215**, 642-652.

Cioni, C., de Merich, D., Cataldi, E. and Cataudella, S. (1991). Fine structure of chloride cells in freshwater- and seawater-adapted *Oreochromis niloticus* (Linnaeus) and *Oreochromis mossambicus* (Peters). *J. Fish Biol.* **39**, 197-209.

Claiborne, J. B., Blackston, C. R., Choe, K. P., Dawson, D. C., Harris, S. P., Mackenzie, L. A. and Morrison-Shetlar, A. I. (1999). A mechanism for branchial acid excretion in marine fish: identification of multiple Na^+/H^+ antiporter (NHE) isoforms in gills of two seawater teleosts. *J. Exp. Biol.* **202**, 315-324.

Claiborne, J. B., Edwards, S. L. and Morrison-Shetlar, A. I. (2002). Acid-base regulation in fishes: cellular and molecular mechanisms. *J. Exp. Zool.* **293**, 302-319.

Dang, Z. C., Lock, R. A. C., Flik, G. and Bonga, S. E. W. (1999). Metallothione in response in gills of *Oreochromis mossambicus* exposed to copper in fresh water. *Am. J. Physiol. Regul. Integr. Comp. Physiol.* **277**, R320-R331.

Edwards, S. L., Tse, C. M. and Toop, T. (1999). Immunolocalisation of NHE3-like immunoreactivity in the gills of the rainbow trout (*Oncorhynchus mykiss*) and the blue-throated wrasse (*Pseudolabrus tetrious*). *J. Anat.* **195**, 465-469.

Edwards, S. L., Wall, B. P., Morrison-Shetlar, A., Sligh, S., Weakley, J. C. and Claiborne, J. B. (2005). The effect of environmental hypercapnia and salinity on the expression of NHE-like isoforms in the gills of a euryhaline fish (*Fundulus heteroclitus*). *J. Exp. Zool.* **303A**, 464-475.

Esaki, M., Hoshijima, K., Kobayashi, S., Fukuda, H., Kawakami, K. and Hirose, S. (2007). Visualization in zebrafish larvae of Na^+ uptake in mitochondria-rich cells whose differentiation is dependent on foxi3a. *Am. J. Physiol. Regul. Integr. Comp. Physiol.* **292**, R470-R480.

Fuji, T., Kasai, A., Suzuki, K. W., Ueno, M. and Yamashita, Y. (2010). Freshwater migration and feeding habits of juvenile temperate seabass *Lateolabrax japonicus* in the stratified Yura River estuary, the Sea of Japan. *Fish. Sci.* **76**, 643-652.

Fujita, S., Kinoshita, I., Takahashi, I. and Azuma, K. (1988). Seasonal occurrence and food habits of larvae and juveniles of two temperate basses in the Shimanto estuary, Japan. *Jpn. J. Ichthyol.* **35**, 365-370.

Hirai, N., Tagawa, M., Kaneko, T., Seikai, T. and Tanaka, M. (1999). Distributional changes in branchial chloride cells during freshwater adaptation in Japanese seabass *Lateolabrax japonicus*. *Zool. Sci.* **16**, 43-49.

Hiroi, J. and McCormick, S. D. (2007). Variation in salinity tolerance, gill Na^+/K^+-ATPase, $Na^+/K^+/2Cl^-$ cotransporter and mitochondria-rich cell distribution in three salmonids *Salvelinus namaycush*, *Salvelinus fontinalis* and *Salmo salar*. *J. Exp. Biol.* **210**, 1015-1024.

Hiroi, J. and McCormick, S. D. (2012). New insights into gill ionocyte and ion transporter function in euryhaline and diadromous fish. *Respir. Physiol. Neurobiol.* **184**, 257-268.

Hiroi, J., Kaneko, T. and Tanaka, M. (1999). *In vivo* sequential changes in chloride cell morphology in the yolk-sac membrane of Mozambique tilapia (*Oreochromis mossambicus*) embryos and larvae during seawater adaptation. *J. Exp. Biol.* **202**, 3485-3495.

Hiroi, J., McCormick, S. D., Ohtani-Kaneko, R. and Kaneko, T. (2005). Functional classification of mitochondrion-rich cells in euryhaline Mozambique tilapia (*Oreochromis mossambicus*) embryos, by means of triple immunofluorescence staining for Na^+/K^+-ATPase, $Na^+/K^+/2Cl^-$ cotransporter and CFTR anion channel. *J. Exp. Biol.* **208**, 2023-2036.

Hiroi, J., Yasumasu, S., McCormick, S. D., Hwang, P.-P. and Kaneko, T. (2008). Evidence for an apical Na–Cl cotransporter involved in ion uptake in a teleost fish. *J .Exp. Biol.* **211**, 2584-2599.

Hootman, S. R. and Philpott, C. W. (1980). Accessory cells in teleost branchial epithelium. *Am. J. Physiol. Regul. Integr. Comp. Physiol.* **238**, R199-R206.

Horng, J.-L., Hawng, P.-P., Shin, T.-H., Wen, Z.-H., Lin, C.-S. and Lin, L.-Y. (2009). Chloride transport in mitochondria-rich cells of euryhaline tilapia (*Oreochromis mossambicus*) larvae. *Am. J. Physiol. Cell Physiol.* **297**, C845-C854.

Hsu, H.-H., Lin, L.-Y., Tseng, Y.-C., Horng, J.-L. and Hwang, P.-P. (2014). A new model for fish ion regulation: identification of ionocytes in freshwater- and seawater-acclimated medaka (*Oryzias latipes*). *Cell Tissue Res.* **357**, 225-243.

Hwang, P. P. and Hirano, R. (1985). Effects of environmental salinity on intercellular organization and junctional structure of chloride cells in early stages of teleost development. *J. Exp. Zool.* **236**, 115-126.

Hwang, P. P. and Lin, L. Y. (2013). Gill ionic transport, acid-base regulation, and nitrogen excretion. In *The Physiology of Fishes 4* (ed. D. H. Evans and J. B. Claiborne), pp. 205-233. Boca Raton, FL: CRC Press.

Inokuchi, M. and Kaneko, T. (2012). Recruitment and degeneration of mitochondrion-rich cells in the gills of Mozambique tilapia *Oreochromis mossambicus* during adaptation to a hyperosmotic environment. *Comp. Biochem. Physiol. A* **162**, 245-251.

Inokuchi, M., Hiroi, J., Watanabe, S., Lee, K. M. and Kaneko, T. (2008). Gene expression and morphological localization of NHE3, NCC and NKCC1a in branchial mitochondria-rich cells of Mozambique tilapia (*Oreochromis mossambicus*) acclimated to a wide range of salinities. *Comp. Biochem. Physiol. A* **151**, 151-158.

Inokuchi, M., Hiroi, J., Watanabe, S., Hwang, P.-P. and Kaneko, T. (2009). Morphological and functional classification of ion-absorbing mitochondria-rich cells in the gills of Mozambique tilapia. *J. Exp. Biol.* **212**, 1003-1010.

Islam, M. S., Yamashita, Y. and Tanaka, M. (2011). A review on the early life history and ecology of Japanese sea bass and implication for recruitment. *Environ. Biol. Fish.* **91**, 389-405.

Ivanis, G., Esbaugh, A. J. and Perry, S. F. (2008). Branchial expression and localization of SLC9A2 and SLC9A3 sodium/hydrogen exchangers and their possible role in acid–base regulation in freshwater rainbow trout (*Oncorhynchus mykiss*). *J. Exp. Biol.* **211**, 2467-2477.

Kato, A., Muro, T., Kimura, Y., Li, S., Islam, Z., Ogoshi, M., Doi, H. and Hirose, S. (2011). Differential expression of Na^+-Cl^- cotransporter and Na^+-K^+-Cl^- cotransporter 2 in the distal nephrons of euryhaline and seawater pufferfishes. *Am. J. Physiol. Regul. Integr. Comp. Physiol.* **300**, R284-R297.

Katoh, F., Hasegawa, S., Kita, J., Takagi, Y. and Kaneko, T. (2001). Distinct seawater and freshwater types of chloride cells in killifish, *Fundulus heteroclitus*. *Can. J. Zool.* **79**, 822-829.

Kinoshita, I., Fujita, S., Takahashi, I., Azuma, K., Noichi, T. and Tanaka, M. (1995). A morphological and meristic comparison of larval and juvenile temperate bass, *Lateolabrax japonicus*, from various sites in western and central Japan. *Jpn. J. Ichthyol.* **42**, 165-171.

Kumai, Y. and Perry, S. F. (2011). Ammonia excretion via Rhcg1 facilitates Na^+ uptake in larval zebrafish, *Danio rerio*, in acidic water. *Am. J. Physiol. Regul. Integr. Comp. Physiol.* **301**, R1517-R1528.

Lee, W., Huang, C.-Y. and Lin, H.-C. (2008). The source of lamellar mitochondria-rich cells in the air-breathing fish, *Trichogaster leeri*. *J. Exp. Zool.* **309A**, 198-205.

Lin, Y. M., Chen, C. N., Yoshinaga, T., Tsai, S. C., Shen, I. D. and Lee, T. H. (2006). Short-term effects of hyposmotic shock on Na^+/K^+-ATPase expression in gills of the euryhaline milkfish, *Chanos chanos*. *Comp. Biochem. Physiol. A* **143**, 406-415.

Lin, T.-Y., Liao, B.-K., Horng, J.-L., Yan, J.-J., Hsiao, C.-D. and Hwang, P.-P. (2008). Carbonic anhydrase 2-like a and 15a are involved in acid-base regulation and Na^+ uptake in zebrafish H^+-ATPase-rich cells. *Am. J. Physiol. Cell Physiol.* **294**, C1250-C1260.

Liu, S.-T., Tsung, L., Horng, J.-L. and Lin, L.-Y. (2013). Proton-facilitated ammonia excretion by ionocytes of medaka (*Oryzias latipes*) acclimated to seawater. *Am. J. Physiol. Regul. Integr. Comp. Physiol.,* **305**, R242-R251.

Liu, S.-T., Horng, J.-L., Chen, P.-Y., Hwang, P.-P. and Lin, L.-Y. (2016). Salt secretion is linked to acid-base regulation of ionocytes in seawater-acclimated medaka: new insights into the salt-secreting mechanism. *Sci. Rep.* **6**, 31433.

Lorin-Nebel, C., Boulo, V., Bodinier, C. and Charmantier, G. (2006). The $Na^+/K^+/2Cl^-$ cotransporter in the sea bass *Dicentrarchus labrax* during ontogeny: involvement in osmoregulation. *J. Exp. Biol.* **209**, 4908-4922.

Marshall, W. S. (2013). Osmoregulation in estuarine and intertidal fishes. *Fish Physiol.* **32**, 395-434.

Marshall, W. S. and Grosell, M. (2006). Ion transport, osmoregulation, and acid-base balance. In *The Physiology of Fishes 3* (ed. D. H. Evans and J. B. Claiborne). pp. 177-230. Boca Raton, FL: CRC Press.

Moorman, B. P., Inokuchi, M., Yamaguchi, Y., Lerner, D. T., Grau, E. G. and Seale, A. P. (2014). The osmoregulatory effects of rearing Mozambique tilapia in a tidally changing salinity. *Gen. Comp. Endocrinol.* **207**, 94-102.

Pelis, R. M., Zydlewski, J. and McCormick, S. D. (2001). Gill Na^+-K^+-$2Cl^-$ cotransporter abundance and location in Atlantic salmon: effects of seawater and smolting. *Am. J. Physiol. Regul. Integr. Comp. Physiol.* **280**, R1844-R1852.

Pisam, M., Prunet, P., Boeuf, G. and Jrambourg, A. (1988). Ultrastructural features of chloride cells in the gill epithelium of the Atlantic salmon, *Salmo salar*, and their modifications during smoltification. *Am. J. Anat.* **183**, 235-244.

Pisam, M., Massa, F., Jammet, C. and Prunet, P. (2000). Chronology of the appearance of beta, A, and alpha mitochondria-rich cells in the gill epithelium during ontogenesis of the brown trout (*Salmo trutta*). *Anat. Rec.* **259**, 301-311.

Sakamoto, T., Kozaka, T., Takahashi, A., Kawauchi, H. and Ando, M. (2001). Medaka (*Oryzias latipes*) as a model for hypoosmoregulation of euryhaline fishes. *Aquaculture* **193**, 347-354.

Sardet, C., Pisam, M. and Maetz, J. (1979). The surface epithelium of teleostean fish gills. Cellular and junctional adaptations of the chloride cell in relation to salt adaptation. *J. Cell Biol.* **80**, 96-117.

Sasai, S., Kaneko, T., Hasegawa, S. and Tsukamoto, K. (1998). Morphological alteration in two types of gill chloride cells in Japanese eel (*Anguilla japonica*) during catadromous migration. *Can. J. Zool.* **76**, 1480-1487.

Scott, G. R., Claiborne, J. B., Edwards, S. L., Schulte, P. M. and Wood, C. M. (2005). Gene expression after freshwater transfer in gills and opercular epithelia of killifish: insight into divergent mechanisms of ion transport. *J. Exp. Biol.* **208**, 2719-2729.

Seidelin, M., Madsen, S. S., Blenstrup, H. and Tipsmark, C. K. (2000). Time-course changes in the expression of Na^+, K^+-ATPase in gills and pyloric caeca of brown trout (*Salmo trutta*) during acclimation to seawater. *Physiol. Biochem. Zool.* **73**, 446-453.

Seo, M. Y., Mekuchi, M., Teranishi, K. and Kaneko, T. (2013). Expression of ion transporters in gill mitochondrion-rich cells in Japanese eel acclimated to a wide range of environmental salinity. *Comp. Biochem. Physiol. A* **166**, 323-332.

Shen, W.-P., Horng, J.-L. and Lin, L.-Y. (2011). Functional plasticity of mitochondrion-rich cells in the skin of euryhaline medaka larvae (*Oryzias latipes*) subjected to salinity changes. *Am. J. Physiol. Regul. Integr. Comp. Physiol.* **300**, R858-R868.

Takei, Y., Hiroi, J., Takahashi, H. and Sakamoto, T. (2014). Diverse mechanisms for body fluid regulation in teleost fishes. *Am. J. Physiol. Regul. Integr. Comp. Physiol.* **307**, R778-R792.

Tang, C.-H., Hwang, L.-Y., Shen, I.-D., Chiu, Y.-H. and Lee, T.-H. (2011). Immunolocalization of chloride transporters to gill epithelia of euryhaline teleosts with opposite salinity-induced Na$^+$/K$^+$-ATPase responses. *Fish Physiol. Biochem.* **37**, 709-724.

Teranishi, K., Mekuchi, M. and Kaneko, T. (2013). Expression of sodium/hydrogen exchanger 3 and cation-chloride cotransporters in the kidney of Japanese eel acclimated to a wide range of salinities. *Comp. Biochem. Physiol. A* **164**, 333-343.

Tipsmark, C. K., Madsen, S. S., Seidelin, M., Christensen, A. S., Cutler, C. P. and Cramb, G. (2002). Dynamics of Na$^+$, K$^+$, 2Cl$^-$ cotransporter and Na$^+$, K$^+$-ATPase expression in the branchial epithelium of brown trout (*Salmo trutta*) and Atlantic salmon (*Salmo salar*). *J. Exp. Zool.* **293**, 106-118.

Uchida, K. and Kaneko, T. (1996). Enhanced chloride cell turnover in the gills of chum salmon fry in seawater. *Zool. Sci.* **13**, 655-660.

Uchida, K., Kaneko, T., Yamauchi, K. and Hirano, T. (1996). Morphometrical analysis of chloride cell activity in the gill filaments and lamellae and changes in Na$^+$,K$^+$-ATPase activity during seawater adaptation in chum salmon fry. *J. Exp. Zool.* **276**, 193-200.

Uchida, K., Kaneko, T., Miyazaki, H., Hasegawa, S. and Hirano, T. (2000). Excellent salinity tolerance of Mozambique tilapia (*Oreochromis mossambicus*): elevated chloride cell activity in the branchial and opercular epithelia of the fish adapted to concentrated seawater. *Zool. Sci.* **17**, 149-160.

van der Heijden, A. J. H., Verbost, P. M., Eygensteyn, J., Li, J., Wendelaar Bonga, S. E. and Flik, G. (1997). Mitochondria-rich cells in gills of tilapia (*Oreochromis mossambicus*) adapted to freshwater or seawater: quantification by confocal laser scanning microscopy. *J. Exp. Biol.* **200**, 55-64.

Varsamos, S., Diaz, J. P., Charmantier, G., Flik, G., Blasco, C. and Connes, R. (2002). Branchial chloride cells in sea bass (*Dicentrarchus labrax*) adapted to freshwater, seawater, and doubly concentrated seawater. *J. Exp. Zool.* **293**, 12-26.

Wang, Y.-F., Tseng, Y.-C., Yan, J.-J., Hiroi, J. and Hwang, P.-P. (2009). Role of SLC12A10.2, a Na-Cl cotransporter-like protein, in a Cl uptake mechanism in zebrafish (*Danio rerio*). *Am. J. Physiol. Regul. Integr. Comp. Physiol.* **296**, R1650-R1660.

Watanabe, S., Niida, M., Maruyama, T. and Kaneko, T. (2008). Na$^+$/H$^+$ exchanger isoform 3 expressed in apical membrane of gill mitochondrion-rich cells in Mozambique tilapia *Oreochromis mossambicus*. *Fish. Sci.* **74**, 813-821.

Wendelaar Bonga, S. E. and Van der Meij, C. J. M. (1989). Degeneration and death, by apoptosis and necrosis, of the pavement and chloride cells in the gills of the teleost, *Oreochromis mossambicus*. *Cell Tissue Res.* **255**, 235-243.

Wendelaar Bonga, S. E., Flik, G., Balm, P. H. M. and Van der Meij, J. C. A. (1990). The ultrastructure of chloride cells in the gills of the teleost *Oreochromis mossambicus* during exposure to acidified water. *Cell Tissue Res.* **259**, 575-585.

Wilson, J. M., Antunes, J. C., Bouça, P. D. and Coimbra, J. (2004). Osmoregulatory plasticity of the glass eel of *Anguilla anguilla*: freshwater entry and changes in branchial ion-transport protein expression. *Can. J. Fish. Aquat. Sci.* **61**, 432-442.

Wu, S.-C., Horng, J.-L., Liu, S.-T., Hwang, P.-P., Wen, Z.-H., Lin, C.-S. and Lin, L.-Y. (2010). Ammonium-dependent sodium uptake in mitochondrion-rich cells of medaka (*Oryzias latipes*) larvae. *Am. J. Physiol. Cell Physiol.* **298**, C237-C250.

Yan, J.-J., Chou, M.-Y., Kaneko, T. and Hwang, P.-P. (2007). Gene expression of Na$^+$/H$^+$ exchanger in zebrafish H$^+$-ATPase-rich cells during acclimation to low-Na$^+$ and acidic environments. *Am. J. Physiol. Cell Physiol.* **293**, C1814-C1823.

Zydlewski, J. and McCormick, S. D. (2001). Developmental and environmental regulation of chloride cells in young American shad, *Alosa sapidissima*. *J. Exp. Zool.* **290**, 73-87.